

STUDIES ON RELEASE OF RIFAMPICIN FROM CHITOSAN-BASED HYDROGEL

LAURA LU CUTURICU,* CEZAR-DORU RADU,* ANDREEA RALUCA RUSU,*
CODRIN LACATUSU,* ANGELA DANILA,* CRISTINA MIHAELA RIMBU,**
CORNELIU MUNTEANU,* BOGDAN ISTRATE,* VIOREL SCRIPCARIU,****
GEANINA FLORENTINA LUPASCU**** and STEFANA LUCA****

*"Gheorghe Asachi" Technical University Iasi, Mangeron Str., 700050, Iasi, Romania

**Iasi University of Life Sciences, 11, M. Sadoveanu Alley, 700490, Iasi, Romania

***"Grigore T. Popa" University of Medicine and Pharmacy,
16, Universităţii Str., 700115, Iasi, Romania

✉ Corresponding author: C.-D. Radu, cezar-doru.radu@academic.tuiasi.ro

Received August 16, 2022

The paper addresses issues related to the administration of Rifampicin (Rif) in the topical therapy of infected wounds. Considering that chitosan (CS), through its own antimicrobial action, would increase the therapeutic action of the antibiotic in the wound, a chitosan hydrogel was developed to incorporate rifampicin. Tests of swelling and porosity showed a hydrogel with high water absorption and established porous morphology. FTIR spectra confirmed the formation of an intermolecular complex between CS and Rif. SEM images illustrated morphologies specific to CS hydrogels and the presence of Rif particles. Thermogravimetric analyses showed specific individual behavior, although mass loss values followed a common general profile. Rif particles included in the pores of the CS hydrogel are a broad-spectrum antimicrobial agent against Gram-positive bacteria, but do not have the same antimicrobial effect against Gram-negative bacteria. The developed CS-based hydrogel has prospects for topical application of Rif in severe chronic wounds.

Keywords: chitosan hydrogel, Rifampicin, swelling degree, porosity, release Rifampicin, antimicrobial activity

INTRODUCTION

Chitosan (CS) is a natural polymer easily obtained by deacetylation of chitin from crustaceans, insects, seafood waste or other animal and plant sources.^{1,2} A form of chitosan is also found in the cell walls of some fungi (class *Zygomycetes*), in green algae (*Chlorella* sp.), yeasts and protozoa.¹ Structurally, chitin is an insoluble linear mucopolysaccharide, consisting of repeated units of N-acetyl-d-glucosamine (Glc N Ac) linked by β -glycosidic bonds (1 \rightarrow 4).³ The structure of chitin is closely related to that of cellulose and can be regarded as cellulose in which the hydroxyl (-OH) at the C-2 position is replaced by an acetamido group (-NHCOCH₃).⁴ CS and its derivatives represent a valuable class of natural biopolymers suitable for a variety of applications in the fields of pharmaceuticals, agriculture, food, textiles, cosmetics, biotechno-

logy, environment *etc.*^{2,5-9} In recent years, chitosan has been one of the preferred candidates in the field of biotechnology, as the chemical and structural versatility of this non-toxic biopolymer (FDA) has inspired researchers to develop new functional models. A current challenge is the use of chitosan in the form of biological ink that can be used in 3D printers to create tissue regeneration matrices that preserve the living properties of organisms.²

Due to the active amino and hydroxyl groups, chitosan can be easily functionalised and converted into products with antimicrobial properties.¹⁰ Positive charges in the amino groups of chitosan interact electrostatically with negatively charged components on the microbial membrane, leading to a blockade of cellular activity and the appearance of a bacteriostatic effect.¹¹

The antimicrobial potential of chitosan is well known, but its antibacterial intensity is influenced by numerous intrinsic and extrinsic factors. Its *in vitro* antimicrobial activity is closely correlated with its type, molecular weight, viscosity, concentration and the type of solvent used. Similarly, the microbial strains against which the test is performed, the environment, pH *etc.* are also important.^{11,12}

In terms of *in vivo* antimicrobial activity, both aerobic and anaerobic bacteria have been found differentially sensitive to the action of chitosan. The molecular weight of chitosan (high (HMW) or low (LMW)) influences the efficiency and antimicrobial mechanisms. Studies have shown that LMW chitosan has the best antimicrobial activity against aerobic bacteria.¹³

It is known that positively charged amino groups of chitosan can damage the membrane/cell wall by electrostatic interaction with negatively charged components on the surface of the microbial cell. HMW chitosan can bind to the porins in the outer membrane (OM) of Gram-negative bacteria and block nutrient exchange, resulting in cell death. LHW chitosan can penetrate the cell wall structure and alter DNA/RNA activity.¹⁴

LMW chitosan has much lower activity against anaerobic bacteria, compared to aerobic ones, which is probably due to the differences in metabolism between aerobic and anaerobic bacteria.¹⁵ The targets of LMW chitosan are the electronegative substances in microbial cells, but these are absent in anaerobic bacteria because the respiratory chain that produces such substances is absent.¹⁶ Under these conditions, LMW chitosan has a reduced ability to act on anaerobic bacteria. However, the mechanisms underlying the antimicrobial activity of this natural polymer are not yet well understood and there is little experimental evidence of interaction between chitosan and the microbial cell.^{17,18}

Based on the medical need to stop the development of wound infections caused by bacteria prone to take up resistance genes or already resistant to antibiotics, we set out to develop and test a chitosan hydrogel that acts as an adjuvant to rifampicin and is suitable for topical application in infected wounds.

Rifampicin is an antibacterial drug used to treat tuberculosis, but is also recommended for the treatment of severe infections caused by intracellular and extracellular bacteria. In general, it is a fat-soluble drug that is well tolerated, but

when administered intravenously and especially orally, it causes a range of side effects, from the most harmless, such as sweating, colouring of body fluids, *etc.*, to symptoms with major consequences: hypersensitivity reactions, thrombocytopenia, haemolysis or liver and kidney dysfunction. Antibiotic resistance and contraindications to combination with other drugs (antifungals, cyclosporine, HIV protease inhibitors) are other factors that limit the administration of rifampicin.¹⁹ To prevent drug resistance, rifampicin is usually combined with other antimicrobial agents.²⁰ Thus, *in vitro* tests showed the efficacy of the combination of tedizolid and rifampicin against MRSA strains,²¹ the combination of imipenem with rifampicin was particularly efficient against multidrug-resistant *Pseudomonas aeruginosa* strains,²² the combination of linezolid and rifampicin was effective against multidrug-resistant *Escherichia coli*, *Pseudomonas aeruginosa* and *Acinetobacter baumannii*.²³ Also, the combinations of colistin/rifampin, rifampin/sulbactam, rifampin/tigecycline and sulbactam/tigecycline showed good *in vitro* activities against extremely drug-resistant *Acinetobacter baumannii* isolates.²⁴

The combination of rifampicin with chitosan would reduce the dose of the antibiotic and thus side effects, while also reducing the risk of antibiotic resistance, extending the range of antimicrobial activity and facilitating local absorption. Rif-functionalised CS hydrogels can be readily used as first-line therapy in infected wounds, so that the synergistic effect of the two antimicrobial structures can prevent the spread of infection and promote healing. The aim of the present research has been to determine the behavior of Rifampicin as a function of the physico-chemical, diffusion and antibacterial properties of the CS hydrogel.

EXPERIMENTAL

Materials

Chitosan (CAS 9012-76-4, with molecular weight 100,000-300,000) was purchased from ACROS Organics. Rifampicin powder was delivered by Antibiotice SA; CH₃OH and C₂H₅OH were of analytical grade and were purchased from Chimreactiv SRL; NaOH was received from S.C. Atochim SRL. Double-distilled water was used in all experiments.

Methods

Preparation protocol of chitosan hydrogel

CS (0.48 g) was weighed and dissolved by magnetic stirring (125 rpm) in 20 mL of 2%

CH₃COOH solution (v/v) at 50 °C for 2 hours, then, 20 mL of NaOH solution (40 g/L) were added to the CS solution under cold stirring for 30 min. The CS gel (NaOH version) was thus obtained.

An amount of 0.48 g of CS was weighed and dissolved in 20 mL of 2% solution of CH₃COOH (v/v) under magnetic stirring (125 rpm) for 3 hours at 50 °C, and then, 20 mL of phosphate buffer saline (PBS) solution, pH=7.4, was added under cold stirring for 6 hours. The chitosan gel (PBS version) was thus obtained.

Phosphate buffered saline (PBS) is a common buffer used at pH 7.4 for biological systems. PBS matches the osmolarity and ionic strength of the human body. The most common protocol to prepare a PBS solution is to dissolve 8.0 g NaCl, 0.20 g KCl, 1.44 g Na₂HPO₄, and 0.240 g KH₂PO₄ to 1.0 L in water.

The introduction of Rif (0.070 g) into the hydrogel was done by two methods:

- in the hydrogel synthesis stage, when CS is mixed with Rif (0.070 g) and NaOH; respectively with PBS;
- by Rif absorption onto the hydrogel from a Rif solution (0.7 g Rif in 50 mL of double-distilled water), where the hydrogel synthesized prior to the absorption stage is stored in the cold for 24 hours.

Determination of swelling degree

The test involved weighing the dry hydrogel under standard conditions of 20 °C and relative humidity (RH) of 65% – to obtain “m dry” from the formula below. The hydrogel was then immersed in 30 mL of cold double-distilled water for 24 hours. After this time, the hydrogel was removed from the water, the excess solution was carefully absorbed with filter paper and the hydrogel was weighed again (“m wet”). The degree of swelling was the calculated by the formula (1):

$$\text{Swelling degree (\%)} = \frac{(m \text{ wet} - m \text{ dry})}{m \text{ dry}} \cdot 100 \quad (1)$$

Determination of hydrogel porosity

Solvent replacement is the main method for determining the porosity; it involves immersing the dried hydrogel in absolute ethanol overnight and then weighing it after ethanol saturation of the surface.^{25,26} The porosity was calculated by the following formula:

$$\text{Porosity} = P = \frac{(M_2 - M_1) \cdot \rho \cdot V}{V} \quad (2)$$

where M₁ is the mass of dry hydrogel and M₂ is the mass of hydrogel after immersion in ethyl alcohol (100%); ρ is the density of absolute ethanol and V is the volume of the hydrogel determined by immersion in hexane, and by difference in a graded cylinder. Porosity as a physical property is dimensionless, or expressed as percentage.

Release kinetics of Rif from the hydrogel

The release kinetics of the drug from the Rif loaded hydrogel samples was observed by introducing the hydrogel samples into the perspiration kit at 37 °C at a

liquor ratio of 1:50 (w/v).²⁷ The experiments were performed in two ways: covering the hydrogel with a porous PU membrane (0.2 micrometers) to limit the burst effect, and without membrane.

For the membrane experiment, the hydrogel loaded with Rif was deposited on a 100% cotton fabric. The membrane was fixed over the hydrogel, which was pressed on the edges with a thermosetting system by lamination (pressing at 120 °C for 5 seconds). A tight sandwich was formed (containing Rif inside the hydrogel), which was deposited in a beaker with the solution of the perspiration kit at 37 °C, the normal temperature of the human body.

For the version without membrane, the hydrogel with Rif was introduced freely (without membrane) into the beaker with the perspiration kit solution, under the same conditions as in the previous version. Hydrogel sample solutions were kept under magnetic stirring at 37 °C and 1 mL solution samples were extracted at various times. The solution samples were analyzed using a Camspec MR01 UV-vis spectrometer (at $\lambda=475$ nm) and the quantities of Rif, M_{t1}, M_{t2}, M_{t3}, ..., were obtained, and the sample extracted after 72 hours was considered as the quantity of drug released at equilibrium, M_∞.

The perspiration kit contained: 0.025 g/L L-histidine monochloride, 1 g/L NaCl, 0.1 g/L Na₂HPO₄, 0.097 g/L lactic acid; calculated at a liquor ratio of 1:50 (w/v), being specific to human dermis at pH=5.5.²⁵

For dosing of the drug, its calibration curve was plotted. As a working protocol, 0.05 g of Rif was dispersed in 500 mL of double-distilled water under magnetic stirring (125 rpm) for 20 minutes; a dispersion of 0.1 mg Rif/mL was obtained. From this vial, amounts of 1, 2, ..., 7, 8 mL were taken and placed in 50 mL vials. Thus-obtained suspensions were subjected to UV-vis spectrophotometry, in the visible range, at wavelength $\lambda = 475$ nm, using a Camspec M501 system.

Morphological analysis of the hydrogel by SEM

For the analysis of the morphology, a Bruker Quanta 200-3D Dual Beam 179 EDS electron microscope was used, with two systems (SEM and focused ion beam). By sending a 180 electron beam on samples, images were obtained with different magnification degrees.

FTIR spectroscopy

FT-IR spectra of CS, Rif and CS-Rif were recorded using a Biorad FT-IR spectrometer FTS 575C, in the range between 4000 cm⁻¹ and 500 cm⁻¹, after 32 scans at a resolution of 4 cm⁻¹. The spectra processing was carried out with the Horizon MB™ FT-IR Software. After each sample scan, a new reference air background spectrum was recorded and the plate was cleaned with isopropyl alcohol prior to placement of the sample.

Thermal analysis

The thermal analyses were performed with a thermogravimetric balance model STA 449F1 Jupiter (Netzsch, Germany). The thermogravimetric balance was calibrated for temperature, based on sensitivity to standard metals (In, Sn, Bi, Zn and Al), from 25 °C to 700 °C. The mass of the samples was between 7 and 10 mg, and the samples were heated at a heating rate of 10 °C/min. Nitrogen was used as a carrier gas, with a flow rate of 50 mL/min and a protective purge with nitrogen (99.9% purity) for thermobalance, with a flow rate of 20 mL/min. The samples were heated in an open Al₂O₃ crucible; Al₂O₃ being taken as a reference material. Data collection was performed using the Proteus® program.

Antibacterial tests

For *in vitro* testing of antimicrobial activity, the Kirby-Bauer disk diffusion method was used, adapted for testing hydrogels. The method is standardized for testing bacterial susceptibility to various antibiotics.²⁶ The antimicrobial potential of rifampicin-loaded chitosan hydrogels was tested against four Gram-positive bacterial strains: *Staphylococcus aureus* ATCC 25923, methicillin-resistant *Staphylococcus aureus* ATCC 33591, methicillin-resistant *Staphylococcus aureus* ATCC 43300, *Streptococcus pyogenes* ATCC 19615 and two Gram-negative strains: *Escherichia coli* ATCC 25922 and *Pseudomonas aeruginosa* ATCC 9027. In the practice of conventional testing, ATCC (American Type Culture Collection) bacterial strains are used as reference.

The testing method consists in placing the test specimens on the surface of solid culture media populated with microbial cultures. For this purpose, bacterial suspensions were prepared in pure culture for

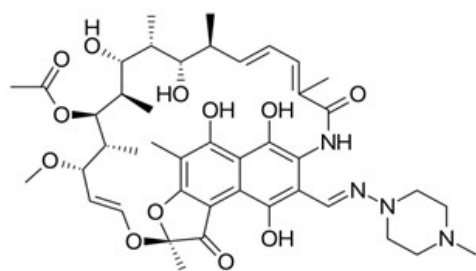


Figure 1: Chemical structure of Rif

Rif is a polyketide that belongs to the chemical class of compounds called ansamycins, so named because of their heterocyclic structure containing a core of naphthoquinone stretched by an aliphatic loop chain. The naphthoquinone chromophore renders rifampicin a crystalline structure with a

specific red-orange color. It is insoluble in water, but soluble in methanol. To avoid possible toxicity in the event of pharmaceutical application, appropriate dosing is important. Therefore, the calibration curve of Rif was determined. To this end, Rif was dispersed in

24 hours, the cell density of which corresponds to the turbidity of the 0.5 McFarland standard (1.5x10⁸ bacterial cells/mL). Then, 1 mL of the bacterial suspension was taken and spread over the surface of the Mueller Hinton Agar (Oxoid) culture medium, previously distributed in 90 mm Petri dishes. After the inoculum was evenly distributed, the bacterial excess was removed and after the surface of the medium dried, the hydrogel + Rif samples were distributed.

Samples of initial CS hydrogel (CS+NaOH), as well as Rif load hydrogel – (CS+NaOH) Rif and (CS+NaOH+Rif), were weighed (7 mg) and modelled in disk form with a diameter of 6 mm. An antibiotic disk (Rifampicin 30 µg) was similarly prepared and used as a positive control.

RESULTS AND DISCUSSION

Considerations regarding Rif and determining its calibration curve

Rifampicin belongs to the pharmacotherapeutic group of medicines for the treatment of tuberculosis – antibiotics with ATC code: J04A B02. A major antituberculous chemotherapeutic, it is a semisynthetic derivative of rifamycin B (antibiotic produced by *Streptomyces mediterranei*). The therapeutic dose in skin infections is 10 mg/kg body weight/24 hours, for two weeks.²⁷ Figure 1 illustrates the chemical structure of Rif.

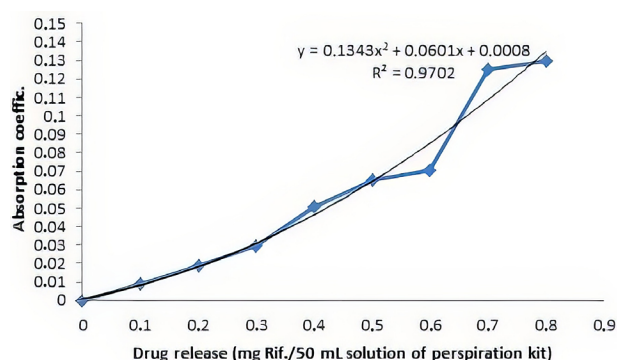


Figure 2: Calibration curve of Rif

Therefore, the calibration curve of Rif was determined. To this end, Rif was dispersed in

double-distilled water and a suspension was obtained, which was subjected to UV-vis spectrophotometry in the visible range, at wavelength $\lambda = 475$ nm, using a Camspec M501 system. The calibration curve of the Rif dispersion is illustrated in Figure 2. Typically, the calibration curve of a product soluble in a liquid medium is obtained by a straight line intersecting the ordinate and the abscissa at zero. As shown in Figure 2 above, the calibration curve is modeled as a second degree equation, which is explained by the fact that the Rif dispersion was mixed in the solution of the perspiration kit for UV-vis spectrophotometry.

Characteristics of CS hydrogel

For the preparation of the hydrogel, an acid solution of 2% CH_3COOH was used in which a quantity of CS (0.48 g) was dissolved by stirring and mild heating for about 2 hours. Under these conditions, the amino groups in CS in the presence of acetic acid pass into ammonium groups, positively charged. After obtaining a clear solution, 20 mL of NaOH (40 g/L) was added under cold stirring. After about 30 minutes of

stirring, a white, consistent and homogeneous compact hydrogel was obtained, which was subsequently tested and was found not soluble in water. The hydrogel was washed with distilled water until a neutral pH was obtained. The amount of NaOH taken up inside the hydrogel was determined by titrating the residual NaOH solution. The presence of sodium cations annihilates the electrostatic rejection of the ammonium groups in the CS, allowing the proximity of the chains, which thus favors the formation of polymer loops with the formation of the hydrogel. However, the presence of NaOH is incompatible with biological applications of the hydrogel. Therefore, the hydrogel was washed in distilled water until a neutral pH was obtained.

The same occurred when in the preparation of the hydrogel, the NaOH solution was replaced with 100 mL PBS, pH = 7.4. The disadvantage of this method, compared to the NaOH process, is the long treatment time – of 6 hours. Table 1 shows the average values of the degree of swelling obtained for the hydrogel calculated by the formula (1).

Table 1
Swelling and porosity values of CS–NaOH hydrogel

No	Mwet (g)	Mdry (g)	Swelling degree (%)	Average (%)
1	10.3039	0.4110	2406	2659.6
2	9.8605	0.3282	2904	
3	8.3617	0.3282	2669	
No	Porosity calculated by formula (2)	Average porosity	Porosity (%) as a function of Mdry	Average (%)
1	0.052	0.073	7.57	9.46
2	0.106		11.35	
3	0.062		9.46	

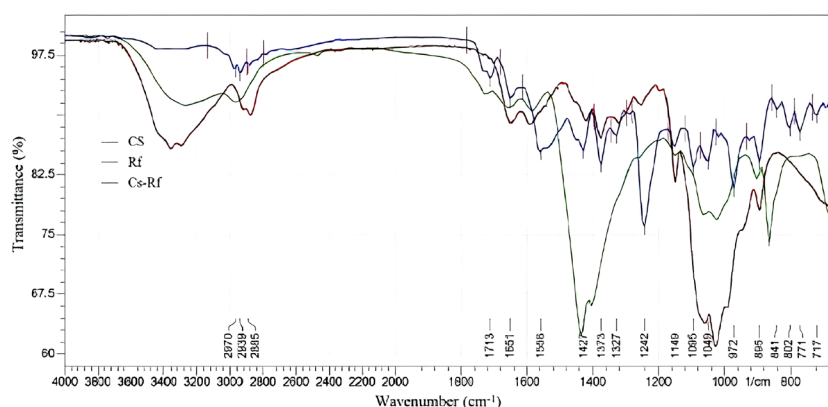


Figure 3: FT-IR spectra of CS, Rif and CS-Rif hydrogel

FTIR spectroscopy

In order to analyze the incorporation of Rif into the CS polymeric matrix, the spectrum of the CS-Rif hydrogel was recorded, along with those of Rif and CS. Figure 3 illustrates the FTIR spectra of CS, Rif, and CS-Rif hydrogel. In the IR spectra of the CS-Rif hydrogel, the characteristic bands of the following functional groups of CS can be observed: at 3296 cm^{-1} ($-\text{NH}_2$), 2920 cm^{-1} ($-\text{OH}$), 1420 cm^{-1} (CH_2) and 1028 cm^{-1} (C-O-C).²⁹⁻³¹ One can also observe the appearance of new absorption bands, specific to Rif, due to its presence in the CS polymeric matrix. The carbonyl ($-\text{C}=\text{O}$) from the ester group of Rif is proved by a narrow absorption band of medium intensity at 1647 cm^{-1} . The presence of a medium intensity absorption band at 1589 cm^{-1} is due to the anti-symmetric stretching vibration of the cumulative double bond ($\text{C}=\text{C}$) from the naphthalene core of Rif. The high and sharp specific absorption band assigned to the methyl group was observed at 1256 cm^{-1} . The amide group is confirmed by the appearance in the IR spectrum of the characteristic bands for $-\text{NH}$ -group at 3364 cm^{-1} .

The formation of an intermolecular complex between CS and Rif, as a result of the electrostatic interaction of the cationic NH_3^+ groups of CS with the anionic ones (five hydroxyl groups, of the ansa bridge and the naphthol ring) of Rif is proved by the presence of the band at 1589 cm^{-1} .

Drug release study

In accordance with the method of obtaining the hydrogel and the inclusion of Rif into it, the following notations were made in the paper:

- (CS+NaOH)+Rif+PU – hydrogel preparation route by mixing CS and NaOH; followed by the introduction of the hydrogel into a Rif solution for 24 hours for Rif absorption into the hydrogel; a polyurethane (PU) membrane was used to cover the hydrogel, which serves to slow down the diffusion of Rif from the hydrogel into the solution of the perspiration kit to reduce the burst effect. The membrane has pores with a diameter of 0.2 microns.

- (CS+NaOH)+Rif – prepared similarly to the previous one, with the difference that it has no PU membrane on the surface and thus the diffusion of the drug into the solution of the perspiration kit is free.

- (CS+NaOH+Rif)+PU – the CS-NaOH hydrogel prepared as described above, but Rif was added during the hydrogel synthesis process; and a PU membrane was applied to slow down the diffusion and reduce the burst effect.

- (CS+NaOH+Rif) – the CS-NaOH hydrogel prepared as described above, with Rif added during the hydrogel synthesis process; no PU membrane was used – the diffusion of the drug was free.

Figures 4-7 illustrate the drug release kinetics for hydrogel formulations studied. The drug release from a hydrogel into a specific environment was modeled using the Korsmeyer-Peppas equation:²⁸

$$\frac{M_t}{M_\infty} = K_{KP} \cdot t^n \quad (3)$$

where M_t and M_∞ are cumulative quantities at time t and at equilibrium (∞); k is a constant related to structural geometric aspects and “ n ” is the exponent of the drug release. This numerical value provides information on the type of diffusion from the hydrogel to the biological interface. Thus, the logarithm form of Equation (3) can be written as follows:

$$\ln\left(\frac{M_t}{M_\infty}\right) = n \cdot \ln t + \ln K_{KP} \quad (4)$$

and Equation (4) becomes the equation of a line where: $y = \ln\left(\frac{M_t}{M_\infty}\right)$, where the slope of the line is n , and x is $\ln t$. The term $\ln K_{KP}$ is a constant, which expresses the magnitude of the line cut. From the experimental data, the values M_{t1} , M_{t2} , *etc.* located on the right side of the experimental curve were used to determine the amount of Rif released at the durations t_1 , t_2 , *etc.* Then, the graph $M_t / M_\infty = f(t)$ was plotted. Subsequently, by graphical representation of the term $\ln\left(\frac{M_t}{M_\infty}\right)$ as a function of $\ln t$, one obtains a line equivalent to Equation (4) whose slope is the release exponent n , as illustrated in Figure 8.

Table 2 presents the specific values of Rif release kinetics. Table 2 compares the specific values of antibiotic release kinetics according to the experiments performed. Thus, for experiments 1 and 3 using the PU membrane, the amounts of drug released at both intermediate times and steady-state durations are lower than in the case of free diffusion, without the use of the membrane (experiments 2 and 4). This means that the membrane has slowed down the diffusion.

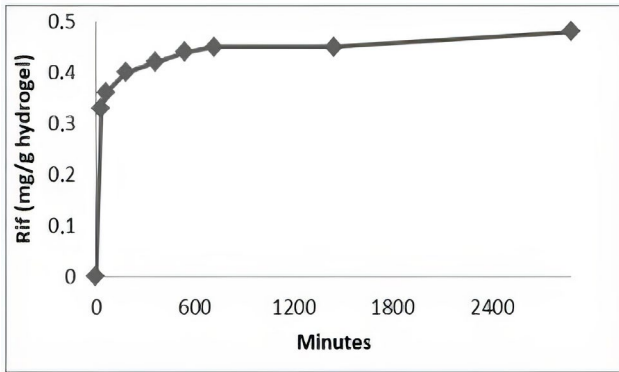


Figure 4: Rif release kinetics from hydrogel (CS + NaOH) Rif PU

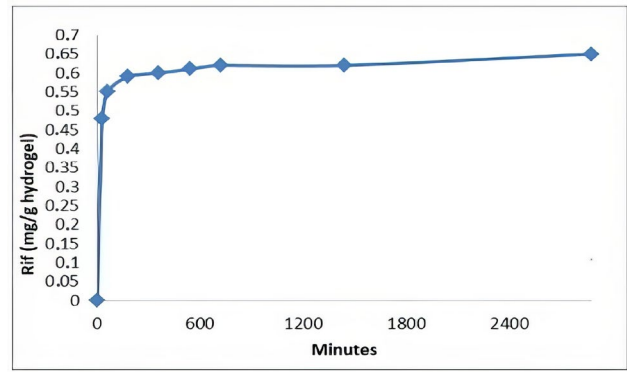


Figure 5: Rif release kinetics from (CS + NaOH) Rif hydrogel

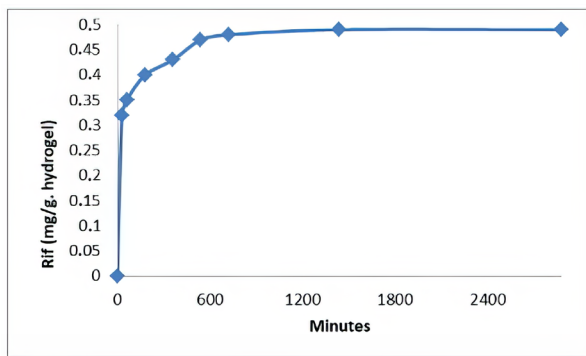


Figure 6: Rif release kinetics from (CS + NaOH + Rif) PU hydrogel

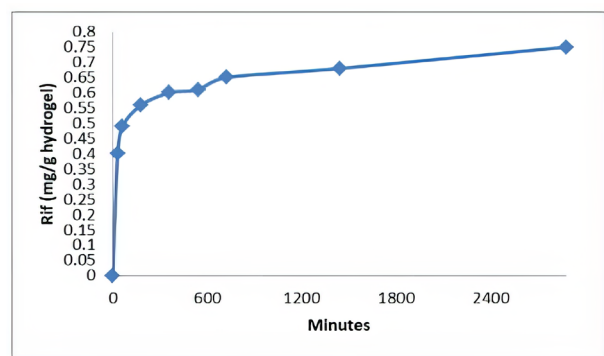


Figure 7: Rif release kinetics from (CS + NaOH + Rif) hydrogel

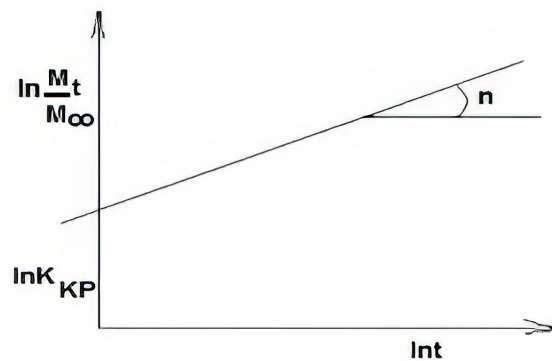


Figure 8: Determination of the Rif release exponent, n, of the Korsmeyer-Peppas Equation (3)

Table 2
Experimental values obtained for Rif release kinetics

Exp.	Formulation	M_{t1}	M_{t2}	M_{∞}	t_1	t_2	n
1	(CS+NaOH)+Rif+PU	0.33	0.36	0.46	30	60	0.76
2	(CS+NaOH)+Rif	0.48	0.55	0.63	30	60	1.58
3	(CS+NaOH+Rif)+PU	0.32	0.35	0.483	30	60	1.05
4	(CS+NaOH+Rif)	0.4	0.49	0.693	30	60	2.04

Table 3
Drug release mechanism according to release exponent values (Korsmeyer-Peppas)

Exp.	n	Transport mechanism of Rif	Speed as a time function
1	0.5	Fickian diffusion	$t^{-0.5}$
2	$0.5 < n < 1.0$	Anomalous transport	t^{n-1}
3	1.0	Case II transport	Zero order release
4	$n > 1$	Super case II transport	t^{n-1}

Table 3 shows literature data³² regarding the interpretation of the transport mechanism as a function of the value of the release exponent, n , from the Korsmeyer-Peppas relation (Eq. 3). The data in Table 2 indicate a decrease in the value of the release exponent for the experiments with the membrane. Thus, it can be stated that in the experiment (CS+NaOH)+Rif+PU, the drug is released through diffusion, which is considered as an anomalous transport of the drug from the hydrogel to the external environment. For the same hydrogel formulation, but in the absence of the outer membrane, the value of n is 1.58, which indicates a super case II transport. For experiments 3 and 4, which are (CS+NaOH+Rif)+PU and (CS+NaOH+Rif), the value of the release exponent also indicates a super case II transport.

In the literature, the conclusions of *in vitro* experiments become theoretical support for anticipating *in vivo* behavior.^{33,34} Modeling drug release is a difficult topic because the properties of the studied system are not stable over time. For example, the formulation of the hydrogel and the phenomena of erosion, organization and relaxation of the polymer chains are decisive factors in the transport mechanism of the drug. Numerous release systems have been characterized using partial differential equations to explain their behavior.³⁵⁻³⁷ Also, empirical and semi-empirical models have been reported in the literature.³⁸⁻⁴⁷ As a general feature of empirical models, it is considered that they cannot explain the full release profile of a system. On the other hand, mathematically supported mechanistic theories take into account specific characteristics of diffusion, erosion, dissolution, *etc.*^{43,48}

The release of a drug from a hydrogel can go through the following stages: i) initial, when a burst effect may occur, in the case of a sudden release of the drug; often the drug readily crosses the hydrogel matrix or, in other cases, the release is delayed; ii) the stage when the hydrogel as a polymeric structure controls the release

mechanism; iii) the rate of drug release decreases as the amount of drug in the hydrogel is depleted.⁴⁹ The steps involved in drug delivery processes are considered to include drug dissolution, diffusion through the hydrogel matrix, swelling or erosion, and transport to the receiving solution at the membrane fluid interface.³⁴ For each model, hypotheses are proposed that establish, as a rule, the correspondence between the mathematical model and the phenomenon studied. However, there is no model that can describe all the problems involved in the release of the drug and, in most cases, this last aspect is not always necessary. When a mathematical model is more general, computational expressions are more difficult, complicating practical applicability. On the other hand, not all aspects of a particular phenomenon are of relatively equal importance. Thus, for models that follow the evolution of drug release, there is a situation when the kinetic behavior of the drug is determined by the swelling or erosion of the polymer, in other cases, the diffusion and dissolution of the drug may play a decisive role. In fact, different mechanisms may occur at the same time or at certain stages during the release process. It is important to establish these mechanisms for the successful design and implementation of controlled release systems, and the identification of potential failure.

Morphological analysis of the hydrogel

The surface morphology of the hydrogel was investigated by SEM and shown in Figures 9-13. The micrographs made at a magnitude of x1000 reveal porous formations specific to a hydrogel. The image in Figure 9 shows the hydrogel formulation that does not contain Rif particles, in contrast to the others (Figs. 10-13). Rif particles appear as white formations on the hydrogel surface, especially on the hydrogels that had a PU membrane. The membrane slowed the diffusion of the drug from the hydrogel, and therefore that the SEM images in Figures 10 and 12 show many

Rif particles present on the surface of the hydrogel. These are visible due to being a dispersion of particles, which are not dissolved in water – this facilitated their visualization through SEM.

Analyzing the micrographs, it may be observed that, in Figure 9, the hydrogel morphology shows exfoliated walls of surface pores. Figure 10 shows the hydrogel surface with associations of Rif particles located at the

interface due to the PU membrane. Figure 11 illustrates a porous surface architecture, with few remaining drug particles; most of them either diffused into the solution of the perspiration kit or remained within the hydrogel. Figure 12 shows a rough surface, with almost horizontal lines, and with antibiotic particles retained on the surface of the PU membrane. In the micrograph in Figure 13, rough wavy morphology is seen, with creases a few microns wide and with Rif particles.

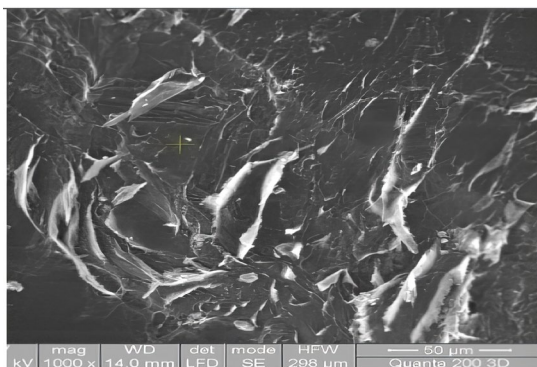


Figure 9: Micrograph of hydrogel (CS+NaOH)

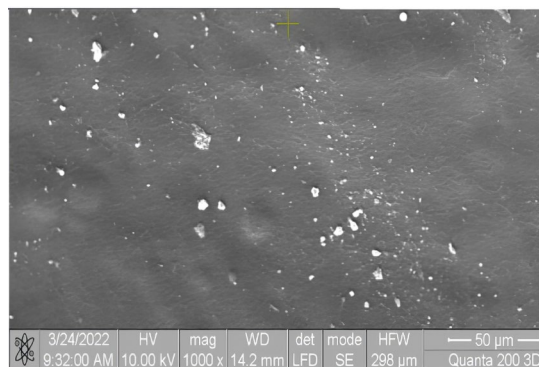


Figure 10: Micrograph of hydrogel (CS+NaOH)+Rif+PU

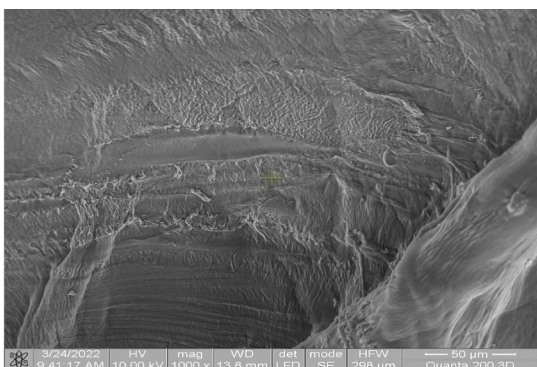


Figure 11: Micrograph of hydrogel (CS+NaOH)+Rif

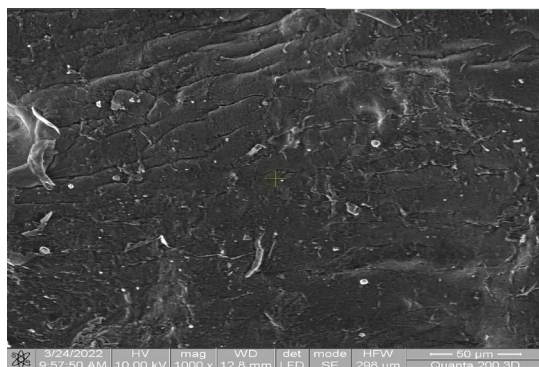


Figure 12: Micrograph of hydrogel (CS+NaOH)+Rif+PU

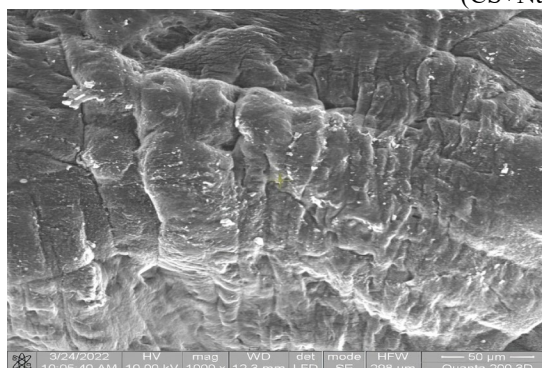


Figure 13: Micrograph of hydrogel (CS+NaOH)+Rif

Thermogravimetric analysis

TG curves were recorded by measuring mass losses between 30 °C and 660 °C. Figure 14

illustrates the TG, DTA and DTG curves for the CS hydrogel sample. Similar curves were obtained for all experiments. Data obtained from

thermogravimetric analyses were plotted in Figure 15.

The main parameters of the degradation processes (T_{onset} – temperature at which thermal degradation begins, T_{peak} – temperature at which the rate of degradation is maximum, T_{20} and T_{30} – temperature at which mass losses of 20% and 30%, respectively, occur; W – weight loss and residue at 650 °C), are summarized in Table 4.

The thermogravimetric data in Figure 15 indicate a relatively close thermal behavior for the analyzed structures. Also, it is observed that, up to the temperature of 250 °C, (CS+Rif+NaOH)+PU presents better thermal stability, compared to the other formulations, after which, the materials show similarity in thermal characteristics.

The degradation of the analyzed formulations over the temperature range of 30-650 °C takes place in 2-5 stages of thermal decomposition. In the first decomposition stage, all the samples exhibit a slight mass loss, of 5-16%, mainly due to the evaporation of adsorbed water ($T_{\text{onset}} = 29\text{-}33$ °C). As the temperature rises above 200 °C, the mass losses are much more significant, being mainly due to the rupture of the OH side groups in the CS and Rif structure, followed by the rupture of the C-C bonds, to initiation, recombination or cyclization reactions and

elimination of gaseous products (CO , CO_2 , NH_3 , aliphatic hydrocarbons and certain carbonyl derivatives), which can contribute to large mass losses.⁵⁰⁻⁵³

The neat CS hydrogel showed in the second stage a mass loss of 55.6% ($T_{\text{onset}} = 201$ °C), while (CS+NaOH) underwent three degradation stages (the first of 12.6%, the second of 37.5% and the third of 16.08%); the total mass losses of the two materials having close values. Also, in the second stage, the mass loss of (CS+NaOH)+Rif+PU reached 53.2% ($T_{\text{init}} = 232$ °C), that of (CS+NaOH)+Rif – 51.4% ($T_{\text{onset}} = 224$ °C). By comparison, (CS+Rif+NaOH)+PU showed in the second stage a mass loss of 39.3% ($T_{\text{onset}} = 245$ °C) and (CS+Rif+NaOH) – a mass loss of 45.54% ($T_{\text{onset}} = 248$ °C).

A special mention should be made regarding hydrogel (CS+Rif+NaOH)+PU, which has 5 stages of degradation. This implies a significant differentiation from the rest of the analyzed samples, and subsequently it may require additional analysis techniques. While the other materials also show some quantitative differences, these are not of special significance, but rather are helpful to differentiate among the various preparation routes.

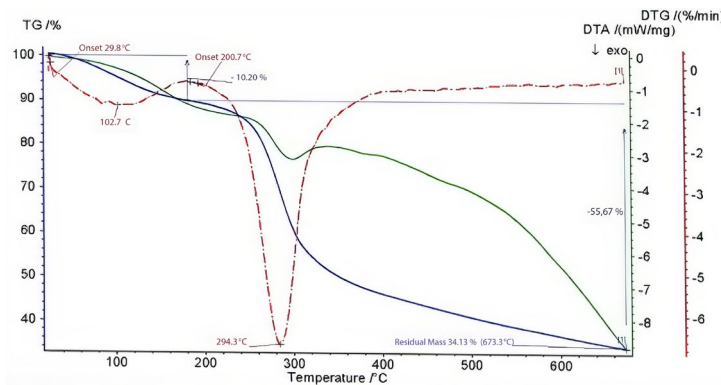


Figure 14: TG, DTA and DTG curves for CS hydrogel

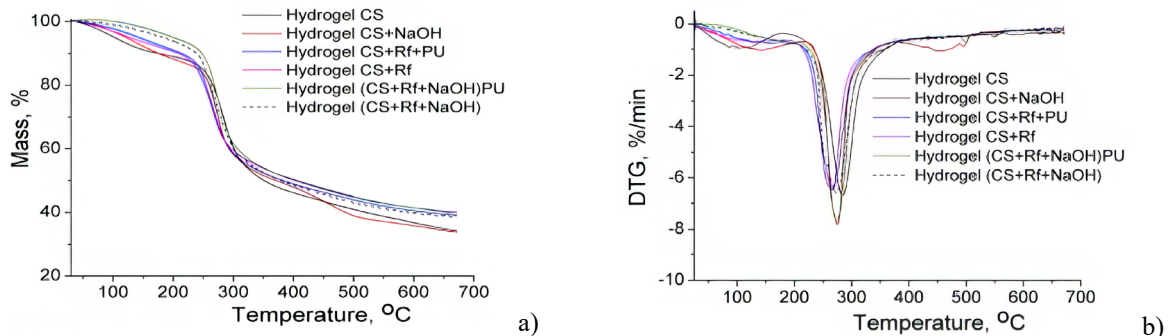


Figure 15: Comparative TG (a) and DTG (b) curves of the materials

Table 4
Thermogravimetric data of hydrogels

Sample	Degradation stage	T _{onset} , °C	T _{peak} , °C	W, %	T ₂₀ , °C	T ₃₀ , °C
1. Hydrogel CS	I	30	103	10.20	266	284
	II	201	284	55.6		
	Residue			34.1		
2. (CS+NaOH)	I	26	146	12.6	261	275
	II	249	276	37.5		
	III	400	451	16.0		
	Residue			33.6		
3. (CS+NaOH)+Rif+PU	I	33	155	8.16	253	270
	II	232	265	53.2		
	Residue			38.8		
4. (CS+NaOH)+Rif	I	35	128	8.5	252	269
	II	224	266	51.4		
	Residue			40.0		
5. (CS+Rif+NaOH)+PU	I	29	-	5.45	269	283
	II	245	272	39.3		
	III	346	353	3.50		
	IV	491	499	7.20		
	V	540	548	5.00		
	Residue			39.3		
6. (CS+Rif+NaOH)	I	33	-	16.2	263	280
	II	248	273	45.5		
	Residue			38.4		

Analyzing the thermal stability of the samples at the temperatures at which the mass losses of 20% and 30% were recorded (Table 4), it can be concluded that the thermal stability increases in the following order: (CS+NaOH)+Rif < (CS+NaOH)+Rif+PU < (CS+NaOH) < (CS+Rif+NaOH) < (CS+Rif+NaOH)+PU < CS.

Antibacterial tests

The antimicrobial potential of the two prototypes of chitosan hydrogel + rifampicin and

the controls of chitosan hydrogel and rifampicin was tested against six reference bacterial strains known for their pathogenicity and effects on human and animal health: *Staphylococcus aureus* ATCC 25923, methicillin-resistant *Staphylococcus aureus* ATCC 33591, methicillin-resistant *Staphylococcus aureus* ATCC 43300, *Streptococcus pyogenes* ATCC 19615, *Escherichia coli* ATCC 25922 and *Pseudomonas aeruginosa* ATCC 9027.

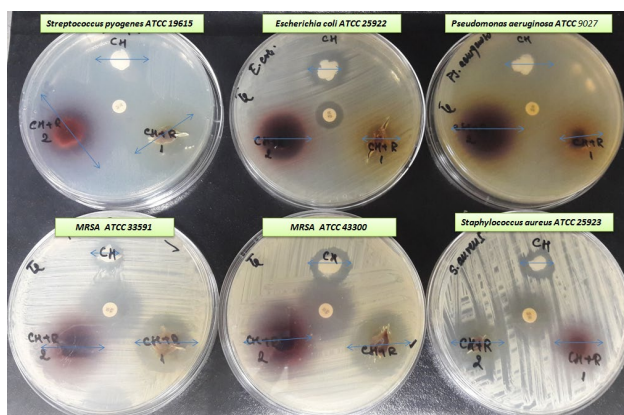


Figure 16: Antimicrobial effect of CS hydrogel (CS+NaOH), hydrogels (CS+NaOH)+Rif and (CS+NaOH+Rif), and Rif (30 µg) against *Streptococcus pyogenes* ATCC 19615; *Escherichia coli* ATCC 25922; *Pseudomonas aeruginosa* ATCC 9027; methicillin-resistant *Staphylococcus aureus* ATCC 33591, methicillin-resistant *Staphylococcus aureus* ATCC 43300, and *Staphylococcus aureus* ATCC 25923

Table 5
Mean inhibition zones (mm) for the investigated samples

Sample (Ø6 mm)	Gram-positive bacteria			Gram-negative bacteria		
	<i>S. aureus</i> ATCC 25923	MRSA ATCC 33591	MRSA ATCC 43300	<i>S. pyogenes</i> ATCC 19615	<i>E. coli</i> ATCC 25922	<i>P. aeruginosa</i> ATCC 9027
	$\bar{X} \pm SE$, mm	$\bar{X} \pm SE$, mm	$\bar{X} \pm SE$, mm	$\bar{X} \pm SE$, mm	$\bar{X} \pm SE$, mm	$\bar{X} \pm SE$, mm
(CS+NaOH)	10.66±0.33	10.76±0.39	16.33±0.33	24.33±0.33	13±1.0	6 ^x
(CS+NaOH)+Rif	20.36±0.31	24.16±0.16	26.9±0.49	35.4±0.30	10±0.11	10.5±0.28
(CS+Rif+NaOH)	26.33±0.88	27.26±0.37	30±0.57	47.43±0.56	20.53±0.29	17.1±0.20
Rif (30 ug)	20	24	22	30	12	6 ^x

^x – without antimicrobial activity; \bar{X} – average; SE – standard error

According to the tests performed, all hydrogel samples were found to have antimicrobial activity against all bacterial cultures tested. The extent of the inhibitory effect was significantly influenced by the composition of the hydrogel and the bacterial strain against which the test was performed (Fig. 16). The antimicrobial activity was evaluated by comparing the average inhibition diameters determined in several tests (Table 5).

The analysis of the data obtained showed that the hydrogel (CS+NaOH+Rif) had the best antimicrobial activity among all the samples tested. The bacterial strains that were most sensitive to (CS+NaOH+Rif) were Gram-positive. Thus, the strongest antimicrobial activity was observed against *Streptococcus pyogenes* (47.43 ± 0.56 mm), followed by methicillin-resistant *Staphylococcus aureus* ATCC 43300 (30 ± 0.57 mm), methicillin-resistant *Staphylococcus aureus* ATCC 33591 (27.26 ± 0.37 mm), and *Staphylococcus aureus* ATCC 25923 (26.33 ± 0.88 mm). Significant antimicrobial activity was also observed against Gram-negative bacterial strains – thus, (CS+NaOH+Rif) showed higher antimicrobial activity values against *Escherichia coli* (20.53 ± 0.29 mm) and *Pseudomonas aeruginosa* (17.1 ± 0.20 mm) than the positive control (Rif).

As for the biological activity of the hydrogel (CS +NaOH)+Rif, it was found that its antimicrobial potential was lower than that of (CS+Rif+NaOH), maintaining the same ratio of antimicrobial activity mainly against Gram-positive bacteria: *Streptococcus pyogenes* (35.4 ± 0.30 mm), methicillin-resistant *Staphylococcus aureus* ATCC 43300 (26.9 ± 0.49 mm), methicillin-resistant *Staphylococcus aureus* ATCC 33591 (24.16 ± 0.16 mm), and *Staphylococcus aureus* (20.36 ± 0.31 mm). The antimicrobial activity against *Escherichia coli* (10

± 0.11 mm) and *Pseudomonas aeruginosa* (10.5 ± 0.28 mm) was significantly reduced.

These results are consistent with others reported in the literature. It is known that rifampicin is a broad-spectrum antimicrobial agent against Gram-positive bacteria, with maximum efficacy against mycobacteria, but does not have the same antimicrobial effect against Gram-negative bacteria.⁵⁴ The antibacterial mechanism of rifampicin is based on the inhibition of bacterial RNA polymerase, the enzyme responsible for DNA transcription.⁵⁵ However, Rifampicin can rapidly induce antimicrobial resistance when administered as such (monotherapy). Combining it with other antimicrobial agents can reduce the occurrence of genetic mutations in the β -subunit of bacterial RNA polymerase (RNAP).⁵⁶ Therefore, its incorporation into a natural matrix with antibacterial properties, such as chitosan, is a viable idea.

Among the tested bacteria, *Pseudomonas aeruginosa* has the highest ability to acquire multiple antibiotic resistance (MDR).⁵⁷ Analysis of the obtained data showed that *Pseudomonas aeruginosa* became susceptible under the action of hydrogels (CS+NaOH)+Rif (10.5 ± 0.28 mm) and (CS+Rif+NaOH) – (17.1 ± 0.20 mm), given that both rifampicin and chitosan hydrogel did not inhibit the culture. These results require further investigation to explain the synergism *in vitro*.

In all other bacterial species, the same antimicrobial effect was observed due to the synergistic effect of rifampicin with chitosan. Of particular importance is the antibacterial activity of these hydrogel prototypes against methicillin-resistant *Staphylococcus aureus* strains. MRSA is one of the most important nosocomial pathogens resistant to antibiotics, which has been associated with surgical wound infections, pneumonia, and sepsis.⁵⁸ The antimicrobial activity of the two

prototypes against these microorganisms is indicative of their applicability to skin infections.

CONCLUSION

In the present study, chitosan-based hydrogels were developed to incorporate rifampicin for antibiotic therapy of infected wounds. The developed hydrogels demonstrated the ability to support the release of Rif. The interaction between NaOH and Rif in the hydrogel formulation did not affect the antistaphylococcal action of the antibiotic. A sensitive point of this application involves intensive washing of the hydrogel before the introduction of Rif into the hydrogel. A version that deserves attention is obtaining the hydrogel using a PBS solution, which, however, requires longer processing times.

Rif is known as being topically effective in skin applications. The developed drug delivery system is a complex diffusion system, where the presence of chitosan is intended to have a synergistic effect with that of rifampicin. Under the experimental conditions presented, the CS hydrogel incorporating Rif formed an intermolecular complex where the ammonium groups of CS and the negative hydroxyl groups of Rif participate ionically. Although a PU membrane was used to slow the diffusion of the drug from the hydrogel to the outer solution, the so-called burst effect was not completely eliminated. The development of the CS and Rif complex system has a therapeutic perspective for the topical application of the antibiotic in severe chronic wounds.

REFERENCES

- D. Raafat and G. Sahl, *Microbiol. Biotechnol.*, **2**, 186 (2009), <https://doi.org/10.1111/j.1751-7915.2008.00080.x>
- M. Taghizadeh, A. Taghizadeh, M. Khodadadi, M. Yazdi, P. Zarrinta *et al.*, *Green Chem.*, **24**, 64 (2022), <https://doi.org/10.1039/d1gc01799c>
- R. N. Tharanathan and S. K. Farooqahmed, *Crit. Rev. Food Sci. Nutr.*, **43**, 61 (2003), <https://doi.org/10.1080/10408690390826455>
- S. Suzuki, *Biotherapy*, **14**, 965 (2000)
- S. Ahmed, M. Ahmad and S. Ikram, *J. Appl. Chem.*, **3**, 493 (2014)
- W. H. Kim, Y. Han, I. S. Lee, N.-I. Wom and Y. H. Na, *Polymer*, **255**, 125112 (2022), <https://doi.org/10.1016/j.polymer.2022.125112>
- P. Rahmani and A. Shojaei, *Polymer*, **254**, 125037 (2022), <https://doi.org/10.1016/j.polymer.2022.125037>
- N. Morin-Crini, E. Lichtfouse, G. Torri and G. Crini, in "Sustainable Agriculture Reviews", Springer International Publishing AG, 2019, pp. 338-341, https://doi.org/10.1007/978-3-030-16538-3_2
- M. M. Koosha, M. Raoufi and H. Moravvejn, *Colloids. Surf. B Biointerfaces*, **179**, 270 (2019), <https://doi.org/10.1016/j.colsurfb.2019.03.054>
- D. Serbezeanu, M. Bercea, M. Butnaru, A. A. Enache and C. M. Rambu, *J. Appl. Polym. Sci.*, **139**, 14 (2022), <https://doi.org/10.1002/app.51912>
- P. Sahariah and M. Måsson, *Biomacromolecules*, **18**, 3846 (2017), <https://doi.org/10.1021/acs.biomac.7b01058>
- Md. S. Z. Rasib, Md. H. Akil, A. Khan and A. Z. A. Hamid, *Int. J. Biol. Macromol.*, **128**, 531 (2019), <https://doi.org/10.1016/j.ijbiomac.2019.01.190>
- E. M. Costa, S. Silva, C. Pina, F. K. Tavarina and M. M. Pintado, *Anaerobe*, **18**, 305 (2012), <https://doi.org/10.1016/j.anaerobe.2012.04.009>
- D. Yan, Y. Li, Y. Liu, N. Li and C. Yan, *Molecules*, **26**, 7136 (2021), <https://doi.org/10.3390/molecules26237136>
- L.-Y. Zheng and J.-F. Zhu, *Carbohydr. Polym.*, **54**, 527 (2003), <https://doi.org/10.1016/j.carbpol.2003.07.009>
- G. Uden and J. Bongaerts, *Biochim. Biophys. Acta*, **1320**, 217 (1997)
- D. Yan, Y. Li, Y. Liu, N. Li and X. Zhang, *Molecules*, **26**, 7136 (2021), <https://doi.org/10.3390/molecules26237136>
- H. Haidari, R. Bright, S. Garg, K. Vasiliev, A. J. Cowin *et al.* *Biomedicines*, **9**, 1182 (2021), <https://doi.org/10.3390/biomedicines9091182>
- A. S. Beloor, A. Rosani and R. Wadhwa, "Rifampin", StatPearls Publishing, 2022, <https://www.ncbi.nlm.nih.gov/books/NBK557488/>
- D. M. Rothstein, *Cold Spring Harb. Perspect. Med.*, **6**, a027011 (2016), <https://doi.org/10.1101/cshperspect.a027011>
- K. Kulthong, S. Srisung, K. Boonpavanitchakul, W. Kangwansupamonkon and R. Maniratanachote, *Part. Fibre Toxicol.*, **7**, 1 (2010), <https://doi.org/10.1186/1743-8977-7-8>
- Laboratory Standards Institute, Antimicrobial Susceptibility Testing Standards M02, M07, and M11; 30th ed., 2020, Wayne, PA, USA, www.nih.org.pk/wp-content/uploads/2021/02/CLSI-2020.pdf
- C. M. Luca, Saint Spiridon University Hospital in Iasi (Romania), Clinic of Infectious Diseases, 2021, personal communication
- N. A. Peppas and B. Narasimhan, *J. Control. Rel.*, **190**, 75 (2014), <https://doi.org/10.1016/j.jconrel.2014.06.041>
- A. Gidari, S. Sabbatini, E. Schiaroli and S. Perito, *Front. Microbiol.*, **11**, 75 (2020), <https://doi.org/10.3389/fmicb.2020.02085> ISSN=1664-302X
- H. F. Hu, C. P. Liu and N. Y. Wang, *BMC Infect. Dis.*, **16**, 444 (2016), <https://doi.org/10.1186/s12879-016-1785-7>

- ²⁷ E. Armengol, T. Asunción, M. Viñas and J. M. Sierra, *Microorganisms*, **8**, 86 (2020), <https://doi.org/10.3390/microorganisms8010086>
- ²⁸ X. Dong, F. Chen and Y. Zhang, *J. Antibiot.*, **67**, 677 (2014), <https://doi.org/10.1038/ja.2014.99>
- ²⁹ C. V. Macarel, Ph.D. Thesis, “Gheorghe Asachi” Technical University Iasi, Romania, 2021, www.tuiasi.ro
- ³⁰ U. Farooq, T. Ahmad, R. Sarwar and J. Shafiq, *Int. J. Nanomed.*, **14**, 3983 (2019), <https://doi.org/doi.org/10.2147/IJN.5198194>
- ³¹ A. Geçer, N. Yıldız and A. Çalmlı, *Macromol. Res.*, **18**, 986 (2010), <https://doi.org/10.1007/s13233-010-1004-0>
- ³² P. Costa and J. M. S. Lobo, *Eur. J. Pharm. Sci.*, **13**, 123 (2001)
- ³³ M. Chorny, I. Fishbein, H. D. Danenberg and G. Golomb, *JCR*, **83**, 389 (2002), [https://doi.org/10.1016/s0168-3659\(02\)00211-0](https://doi.org/10.1016/s0168-3659(02)00211-0)
- ³⁴ A. I. Romero, M. Villegas and A. G. Cid, *Asian J. Pharm. Sci.*, **13**, 54 (2018), <https://doi.org/doi.org/10.1016/j.ajps.2017.08.007>
- ³⁵ A. Siepmann and A. Göpferich, *Adv. Drug. Deliv. Rev.*, **48**, 229 (2001), [https://doi.org/10.1016/s0169-409x\(01\)00116-8](https://doi.org/10.1016/s0169-409x(01)00116-8)
- ³⁶ J. Siepmann and F. Siepmann, *JCR*, **161**, 351 (2012), <https://doi.org/10.1016/j.jconrel.2011.10.006>
- ³⁷ S. Mitragotri, Y. G. Anissimov and A. Bunge, *Int. J. Pharm.*, **418**, 115 (2011), <https://doi.org/10.1016/j.ijpharm.2011.02.023>
- ³⁸ T. Higuchi, *J. Pharm. Sci.*, **50**, 874 (1961)
- ³⁹ R. W. Korsmeyer, R. Gurny and E. Doelker, *Int. J. Pharm.*, **15**, 25 (1983)
- ⁴⁰ P. L. Ritger and N. A. Peppas, *JCR*, **5**, 23 (1987)
- ⁴¹ J. Siepmann and N. A. Peppas, *Adv. Drug. Deliv. Rev.*, **64**, (Suppl.) 163 (2001), [https://doi.org/10.1016/s0169-409x\(01\)00112-0](https://doi.org/10.1016/s0169-409x(01)00112-0)
- ⁴² J. Siepmann, R. A. Siegel and M. J. Rathbone, “Fundamentals and Applications of Controlled Release Drug Delivery”, Springer, New York, 2012, pp. 131-149
- ⁴³ J. Siepmann and F. Siepmann, *Int. J. Pharm.*, **364**, 328 (2008)
- ⁴⁴ J. Crank, “The Mathematics of Diffusion”, Oxford Clarendon Press, 1975
- ⁴⁵ J. M. Vergnaud, “Controlled Drug Release of Oral Dosage Forms”, Taylor and Francis, 1993
- ⁴⁶ J. M. Vergnaud and I. D. Rosca, “Assessing Bioavailability of Drug Delivery Systems: Mathematical Modeling”, CRC Press, 2005
- ⁴⁷ F. Lecomte, J. Siepmann and M. Walther, *Pharm. Res.*, **22**, 1129 (2005), <https://doi.org/10.1007/s11095-005-5421-2>
- ⁴⁸ J. Siepmann, H. Kranz, R. Bodmeier and N. A. Peppas, *Pharm. Res.*, **16**, 1748 (1999), <https://doi.org/10.1023/a:1018914301328>
- ⁴⁹ C. K. Sackett and B. Narashim, *Int. J. Pharm.*, **418**, 104 (2011), <https://doi.org/10.1016/j.ijpharm.2010.11.048>
- ⁵⁰ N. Tudorachi, A. P. Chiriac, L. Niță and F. Mustață, *J. Therm. Anal. Calorim.*, **131**, 1867 (2018), <https://doi.org/10.1007/s10973-017-6682-9>
- ⁵¹ N. Tudorachi and F. Mustață, *J. Therm. Anal. Calorim.*, **119**, 1703 (2015), <https://doi.org/10.1007/s10973-014-4320-3>
- ⁵² R. Rotaru, M. Savin, N. Tudorachi, C. Peptu, P. Samoila *et al.*, *Polym. Chem.*, **7**, 860 (2018), <https://doi.org/10.1039/C7PY01587A>
- ⁵³ A. P. Chiriac, A. Rusu, L. E. Tudorachi, A. Diaconu, D. Rusu *et al.*, *Rev. Roum. Chim.*, **63**, 673 (2018)
- ⁵⁴ H. G. Floss and T. W. Yu, *Chem. Rev.*, **105**, 621 (2005), <https://doi.org/10.1021/cr030112j>
- ⁵⁵ E. A. Campbell, N. Korzheva, A. Mustaev, K. Murakami, S. Nair *et al.*, *Cell*, **104**, 901 (2001), [https://doi.org/10.1016/S0092-8674\(01\)00286-0](https://doi.org/10.1016/S0092-8674(01)00286-0)
- ⁵⁶ B. P. Goldstein, *J. Antibiot.*, **67**, 625 (2014), <https://doi.org/10.1038/ja.2014.107>
- ⁵⁷ Z. Pang, R. Raudonis, B. R. Glick, T.-J. Lin and Z. Cheng, *Biotechnol. Adv.*, **37**, 177 (2019), <https://doi.org/10.1016/j.biotechadv.2018.11.013>
- ⁵⁸ J. Larsen, C. L. Raisen and X. Ba, *Nature*, **602**, 135 (2022), <https://doi.org/10.1038/s41586-021-04265-w>